



Cite this: *Green Chem.*, 2016, **18**, 2155

Towards quantitative and scalable transformation of furfural to cyclopentanone with supported gold catalysts†

Gao-Shuo Zhang, Ming-Ming Zhu, Qi Zhang, Yong-Mei Liu, He-Yong He and Yong Cao*

Given the vital importance of furfural (FFA) upgrading towards a sustainable bio-based economy, an eco-friendly aqueous route to produce a sole valuable product from FFA is highly desirable. We herein describe an efficient approach to quantitatively convert FFA into cyclopentanone (CPO) in neat water, employing H₂ as the clean reductant and supported gold nanoparticles as a simple yet versatile catalyst. The use of anatase TiO₂ featuring only mild Lewis acidic sites as the underlying support is essential, not only for preventing undesirable side reactions, but also for attaining high CPO selectivity. The feasibility of using biogenic CPO and CO₂ as benign carbon sources to synthesize the industrially important feedstock dimethyl adipate is also demonstrated.

Received 21st October 2015,
Accepted 26th November 2015

DOI: 10.1039/c5gc02528a

www.rsc.org/greenchem

Introduction

The last two decades have witnessed a spectacular surge in the utilization of renewable resources as chemical feedstocks for the development of sustainable chemical processes.¹ In this respect, furfural (FFA) is an important renewable C₅ resource, which is considered to be one of the key platform molecules derived from lignocellulosic biomass and is already used as a raw material for the production of important industrial chemicals in certain cases.² While significant recent efforts have been directed at exploiting new innovative catalytic routes and processes to convert furfural into various high-density bio-synthetic fuels, the development of novel transformations that can expand the existing methods for practical and cost-effective furfural upgrading is still a very important topic of huge industrial interest.³ Aqueous-phase hydrogenative rearrangement of FFA is particularly attractive in this regard since it offers a clean and sustainable alternative to access cyclopentanone (CPO),⁴ a very useful compound under heavy demand but which still relies exclusively on fossil-based feedstocks (Scheme 1a).⁵ Given the vital importance of CPO and its derivatives, which are not only applied in current pharmaceuticals but also used as versatile intermediates in the preparation of fungicides, flavors, rubber chemicals and functionalized

materials (Scheme 1c),^{4c} the identification of new efficient routes pertaining to its straightforward and targeted production from renewable sources has become essential.^{4,5}

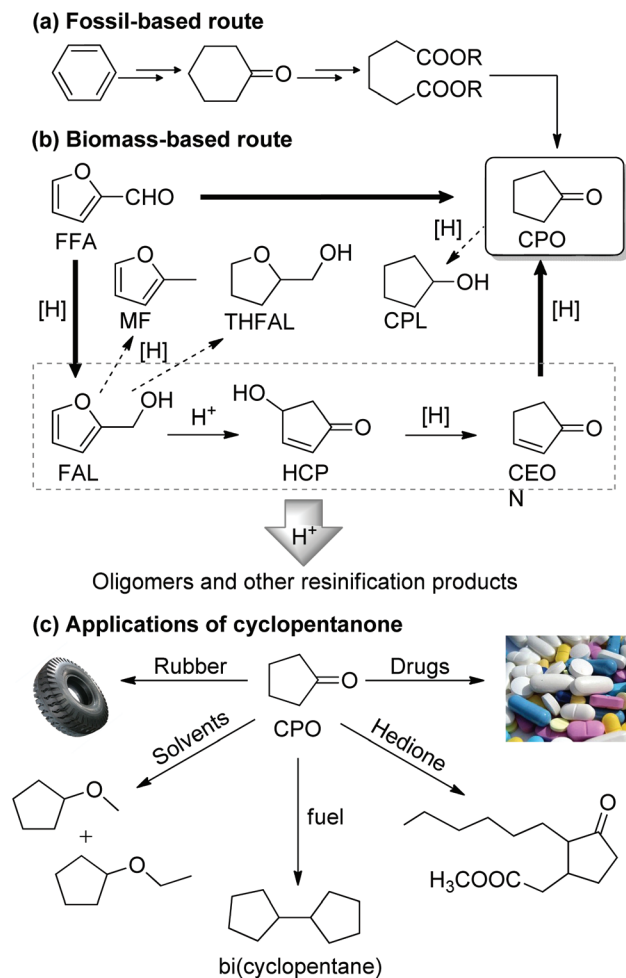
Although the related transformations for preparing CPO derivatives by an acid-catalyzed rearrangement of suitable 2-furylcarbinols have been known for nearly 4 decades,⁶ only very recently selective catalytic systems have appeared for direct conversion of FFA into CPO, pioneered by the group of Hronec *et al.*^{4a,b} A crucial issue for this particular transformation is the large variety of reduction products that can possibly be formed (Scheme 1b). Besides CPO, cyclopentanol (CPL), furfuryl alcohol (FAL), and tetrahydrofurfuryl alcohol (THFAL) are also typically formed during the FFA reduction. An additional challenge lies in the fact that considerable resinification may readily occur during the reaction,⁴ and this could ultimately lead to an unacceptable product loss and in turn a fast catalyst deactivation. So far, a plethora of supported Group VIII and IB metal catalysts have been explored in the selective production of CPO from FFA.⁴ However, with these catalysts it has proven difficult to achieve the desired selectivities, particularly at high conversion levels. Most recently, the use of an acidic metal-organic framework (MOF) supported Ru enabling CPO yields higher than 95% was described,^{4h} but the limited turnover numbers (TONs < 2000) and inherently labile nature of the MOF-based material have precluded its potential utility in a biorefinery. Consequently, catalytic FFA-to-CPO transformation in a highly selective, efficient, robust and scalable manner still remains a pending challenge.

Heterogeneous reduction catalyzed by supported gold nanoparticles (NPs) has emerged over the past several years as a

Department of Chemistry, Shanghai Key Laboratory of Molecular Catalysis and Innovative Materials, Fudan University, Shanghai 200433, P. R. China.

E-mail: yongcao@fudan.edu.cn; Fax: (+86-21) 65643774

† Electronic supplementary information (ESI) available. See DOI: 10.1039/c5gc02528a



Scheme 1 The current and "future" processes for CPO production.

powerful tool for clean chemical production. A set of recent papers exploring the potential of Au-catalyzed reductions,⁷ together with our contributions to this field,⁸ exemplify successful applications of supported gold in a wide variety of substrates, such as nitro compounds, alkynes, quinolines and in particular unsaturated aldehydes. Notwithstanding the significant progress to date, a key factor impeding the wider adoption of Au-catalyzed reduction protocols is the lack of a potent catalyst capable of efficient and reliable operation with very high TONs at a level amenable to large-scale applications. Herein for the first time, we report a highly versatile gold-catalyzed FFA reduction system, in which the reaction can be driven toward the exclusive formation of CPO. With this system, TONs approaching 1.0×10^6 were possible for converting FFA. Crucial for this unique selectivity and unprecedented high productivity is the optimal control of the metal–acid balance in the bifunctional Au/TiO₂ catalysts to prevent unwanted resinification processes, which prevailed in previous FFA hydrogenation/rearrangement reactions.^{4a–c} Additionally, we demonstrate the possibility of converting biogenic CPO and benign dimethyl carbonate (DMC) into industrially important dimethyl adipate (DAP) under clean and mild conditions.

Results and discussion

Building upon previous studies signifying the importance of an acidic environment for a Piantcatelli rearrangement,^{4,6} our initial catalyst development efforts focused on the use of a range of solid acidic materials as the supports to explore the feasibility of converting FFA into CPO *via* Au-catalyzed selective hydrogenation in neat water under batch conditions (Table 1). For these preliminary assays, the conditions studied were 160 °C, 4 MPa H₂, 0.5 M aqueous FFA and with a substrate/Au (S/C) ratio of 2000:1, wherein the extremely low catalyst loading employed is noteworthy. Unfortunately, it turns out that these screening reactions were plagued by the formation of large amounts of insoluble brown solids resulting in considerable carbon loss. In particular, when the reaction was performed with a highly acidic Nb₂O₅ supported Au catalyst (Au/Nb₂O₅), FFA was polymerized severely and almost no CPO (entry 1) was produced, despite the reported effectiveness of this material in the conversion of 5-hydroxymethylfurfural to a cyclopentanone derivative.⁹ Such a pronounced lack of mass balance is clearly the effect of an unfavourable proton-mediated intermolecular resinification associated with these screening assays, in line with previous observations made by Hronec *et al.*⁴ This scenario, together with the unsuccessful attempts to rely upon other acidic carriers (entries 2 and 3), underscored the need to explore alternative support materials.

As a result of conventional strong solid acids not being able to promote the required FFA conversion, we considered the possibility of using solid supports possessing lower acidity to suppress the undesired side reactions. Selected examples of such types of supporting materials that were surveyed are shown in Table 1. At this stage we focused primarily on the outcomes resulting from several ubiquitous metal-oxide supports featured with medium-strength Lewis acidity and weak Brønsted acidity. Our studies revealed that, upon using SiO₂, ZrO₂, and Al₂O₃, the selectivity to CPO and CEON significantly increased and an excellent mass balance could be obtained when applying various polymorphs of TiO₂ as a support (entries 7–9). Gratifyingly, Au deposited on a single-phase anatase (Au/TiO₂-A) was uniquely effective in promoting the quantitative FFA-to-CPO transformation with essentially no other side products observed (Table 1, entry 9). The success of this gold-TiO₂-A combination for this complex multistep reaction was somewhat surprising as anatase TiO₂ possesses only weak Lewis acidic sites.¹⁰ This fact and the observed inhibition of the reaction by introducing either mineral acid or base additives (see Table S1†) demonstrate that both strongly acidic and basic conditions have a strong detrimental effect on the desired catalytic performance.

The enabling capabilities for directing the reaction pathways in a highly target-oriented manner by this Au/TiO₂-A system over related catalyst systems are apparent from a comparison of their kinetic profiles for the hydrogenation of FFA. In contrast to the sluggish and complex kinetics of the FFA-to-CPO conversion occurring with other systems (Fig. 1a and b), the conversion of FFA with Au/TiO₂-A proceeds smoothly and

Table 1 Hydrogenative rearrangement of FFA to CPO over different catalysts^a

Entry	Catalyst ^b	S/C ^c	<i>t</i> [h]	Conv. ^d [%]	Mass balance [%]	Sel. ^d [%]				
						CPO	CPL	MF	FAL	CEON
1	Au/Nb ₂ O ₅ (0.61 wt%)	2000	3	51	24 ± 5	8	2	0	9	5
2	Au/H-ZSM-5 (0.62 wt%)	2000	3	42	44 ± 4	17	1	0	15	11
3	Au/HY (0.64 wt%)	2000	3	47	35 ± 4	11	0	0	14	10
4	Au/ZrO ₂ (0.68 wt%)	2000	1.2	49	72 ± 3	59	1	11	0	1
5	Au/SiO ₂ (0.65 wt%)	2000	1.2	43	94 ± 2	41	0	0	11	42
6	Au/Al ₂ O ₃ (0.85 wt%)	2000	1.2	46	96 ± 2	52	0	0	6	38
7	Au/TiO ₂ -R (0.63 wt%)	2000	1.2	46	99 ± 1	69	0	0	0	31
8	Au/TiO ₂ -P25 (0.62 wt%)	2000	1.2	72	99 ± 1	74	0	0	0	26
9	Au/TiO ₂ -A (0.73 wt%)	2000	1.2	>99	99 ± 1	>99	0	0	0	0
10	Au/TiO ₂ -A (0.24 wt%)	2000	1.2	>99	99 ± 1	>99	0	0	0	0
11	Au/TiO ₂ -A (0.10 wt%)	2000	1.2	>99	99 ± 1	>99	0	0	0	0
12	Au/TiO ₂ -A (0.73 wt%)	10 000	7	94	96 ± 2	96	0	0	0	0
13	Au/TiO ₂ -A (0.24 wt%)	10 000	7	97	98 ± 2	98	0	0	0	0
14	Au/TiO ₂ -A (0.10 wt%)	10 000	7	>99	99 ± 1	>99	0	0	0	0
15 ^e	Au/TiO ₂ -A (0.10 wt%)	20 000	14	>99	99 ± 1	>99	0	0	0	0
16 ^{e,f}	Au/TiO ₂ -A (0.10 wt%)	20 000	15	99	99 ± 1	>99	0	0	0	0

^a Reaction conditions: FFA (5.2 mmol), H₂O (10 mL), H₂ (4 MPa), 160 °C. ^b The preparation procedure for all catalysts and relevant characterization data are provided in the ESI. The values given in parenthesis represent the weight content of the active metal deposited on solid supports. ^c S/C = substrate-to-catalyst molar ratio. ^d Determined using a GC/MS-based method. ^e FFA (50 mmol), H₂O (100 mL), H₂ (4 MPa), 160 °C. ^f The 5th reuse of the catalyst recovered from entry 15.

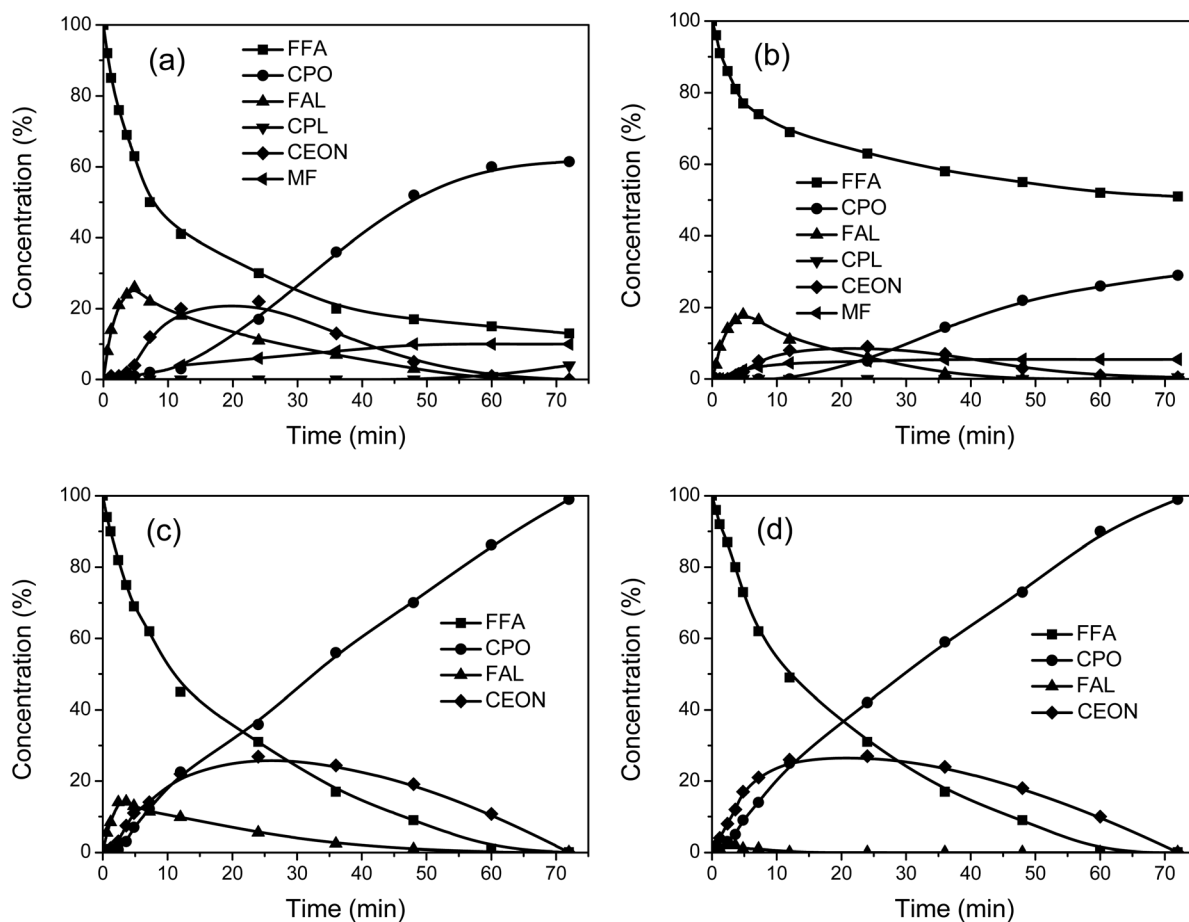


Fig. 1 Reaction profiles for the hydrogenation of FFA over various catalysts at a metal loading of 0.05 mol% (S/C ~ 2000). (a) 0.73 wt% Pt/TiO₂-A (b) 0.68 wt% Au/ZrO₂ (c) 0.73 wt% Au/TiO₂-A. (d) 0.10 wt% Au/TiO₂-A. Reaction condition: FFA (5.2 mmol), H₂O (10 mL), H₂ (4 MPa), 160 °C.

reaches complete conversion after approximately 1.2 h at 160 °C (Fig. 1c), with no competitive formation of resinous products to any degree. This observation appears to be striking given that the key intermediate FAL is in fact highly prone to experiencing intermolecular aldol condensation, dehydration or hydrolysis side reactions that can lead to the formation of complex oligomers,⁴ as verified by a set of control experiments employing various concentrations of aqueous FAL as the starting materials (Fig. 2). Importantly, these results highlight the imperative need for maintaining a sufficiently low level of FAL in the reaction medium to minimize the formation of by-products arising from resinification. The exclusive formation of the CPO product can thus be readily rationalized by a significantly reduced FAL accumulation enabled with Au/TiO₂-A even at the early stages of the reaction, along with a subsequent preferential reduction of the C=C moiety in the rearrangement product of CEON (Fig. 1c).

A crucial advantage of the Au/TiO₂-A system is therefore the potential to manipulate this reaction in such a way as to “switch off” unwanted side reactions. As a further illustration of the benefits of this previously unappreciated Au–TiO₂-A combination for furnishing the desired CPO, attempted platinum-group-metal (PGM)-based catalysts using TiO₂-A decorated with Pt, Pd, Ir or Rh NPs can only afford a much less selective and very limited FFA-to-CPO conversion under otherwise identical conditions (Table S2†),¹¹ despite the widely recognized effectiveness of these metals in hydrogenation reactions.¹² To gain an insight into the underlying causes of this remarkable Au-support synergy, we were prompted to evaluate the possible functional significance of each of the key components in the Au/TiO₂-A system. To this end, a systematic study of a set of Au/TiO₂-A-based materials with varied gold loadings and different-sized Au particles was carried out. It was clarified that the adoption of small Au NPs (<3 nm) is essential for efficient reductive conversion of FFA (Table S4†). However, perhaps the most noteworthy finding was that the initial transient FAL buildup can be greatly inhibited by decreasing the gold loading down to 0.10 wt% (Fig. 1d).

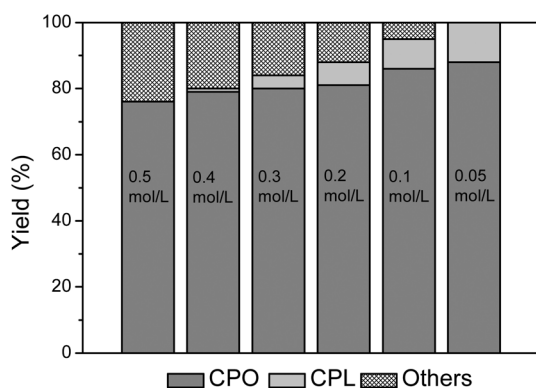


Fig. 2 Hydrogenative transformation of FAL over various concentration with 0.73 wt% Au/TiO₂-A. Reaction conditions: S/C (2000), H₂ (4 MPa), 160 °C, 0.6 h.

Coupled with almost the same FAL evolution kinetics in association with a physical mixture of 0.73 wt% Au/TiO₂-A and bare TiO₂-A (Fig. S1b†), these results illustrate that an optimal combination of Au-support cooperation, in which Au furnishes suitable hydrogenation activity and anatase TiO₂ affords mild water-compatible Lewis acid sites in close vicinity to the Au species, is essential for steering the reaction toward the desired product in an entirely exclusive manner.

The 0.10 wt% Au/TiO₂-A material turned out to be more effective than other Au/TiO₂-A-based samples in terms of yielding CPO quantitatively at a Au loading level as low as 0.01 mol% (Table 1, entry 14). Upon close inspection of the product evolution as shown in Fig. 3, one can readily recognize that the CEON hydrogenation is the rate-determining step of the overall reaction in the present Au-catalyzed system. In an investigation into the effect of reaction parameters on the performance of the 0.10 wt% Au/TiO₂-A catalyst, operation at 160 °C and a H₂ pressure of 4 MPa were found to be optimal (Table S5†). Additionally, it was verified that nearly quantitative CPO yields can also be achieved for a concentrated aqueous solution of FFA (ca. 30 wt%), confirming the remarkable potential of this system for FFA upgrading (Table 2). Further-

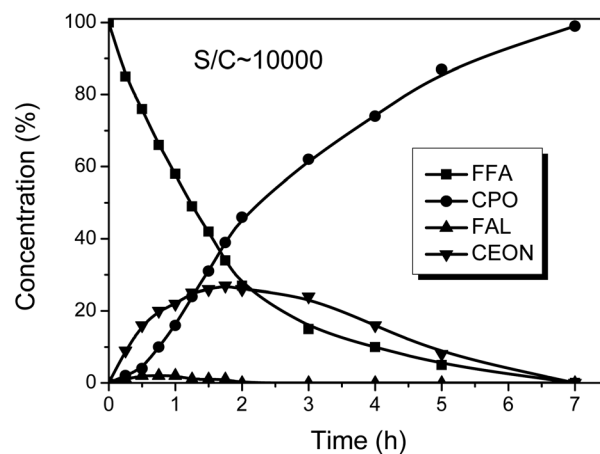


Fig. 3 Kinetic time course of the FFA-to-CPO transformation in the presence of 0.10 wt% Au/TiO₂-A, with only a trace amount of FAL identified as the intermediate. Reaction conditions: H₂O (10 mL), H₂ (4 MPa), 160 °C, with FFA (5.2 mmol) at a S/C ratio of 10 000 : 1.

Table 2 The effect of the concentration of FFA over 0.10 wt% Au/TiO₂-A^a

Entry	H ₂ O [mL]	FFA [mmol]	Mass balance [%]	Yield ^b [%]
1	10	5.2	99 ± 1	99
2	5	5.2	99 ± 1	99
3	2.5	5.2	98 ± 2	98
4 ^c	2.5	10.4	92 ± 2	92

^a Reaction conditions: S/C (2000), H₂O (10 mL), H₂ (4 MPa), 160 °C, 1.2 h. ^b The yield was based on CPO. ^c 2.5 h.

more, this new Au-catalyzed hydrogenation/rearrangement methodology can be readily extended to fabricate a variety of substituted cyclopentanones from other furan-based derivatives. For example, when 2-acetylfuran and 2-propionylfuran were exposed to these new reductive conditions, the resultant 2-methylcyclopentanone and 2-ethylcyclopentanone could be obtained in nearly quantitative yields, respectively. Interestingly, direct reaction of 5-methylfurfural or 5-ethylfurfural also furnishes their corresponding alicyclic derivatives in high yields (Table 3). This is somewhat unexpected, given the absence of a substituent at the 5-position of the furan ring is known to be a critical prerequisite for the intramolecular Pinnacelli type rearrangement,^{6a-b} but this can be justified by the fact that the Lewis acid sites on TiO₂ can facilitate the rearrangement of 5-substituted furan derivatives.¹³

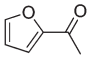
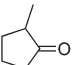
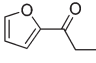
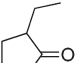
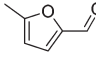
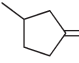
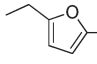
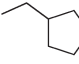
To further evaluate the catalytic activity of 0.10 wt% Au/TiO₂-A, we performed a series of kinetic measurements with FFA as a substrate on a 50 mmol scale (Fig. S4†). At an even lower loading of 0.005 mol% of Au (S/C of 20 000), a high conversion of 99% was still achievable, although a longer reaction time is required (entry 15). In these experiments, the initial reaction rates were found to be linearly dependent on the catalyst concentration (Fig. S5†), consistent with a situation where the reaction follows a first-order kinetics with respect to the associated catalyst. Furthermore, although various catalyst systems have often been reported to suffer from the problem of decreasing reusability,^{4e-h} the 0.10 wt% Au/TiO₂-A recovered after its first use in the hydrogenation of FFA was successfully used in five subsequent reactions with no reduction in the reaction rate: the total TON based on Au was greater than 110 000 (Table 1, entry 16). Already, this result represents the best catalyst productivity ever reported for any gold-catalyzed hydrogenations.^{7,8} X-ray diffraction (XRD), transmission electron microscopy (TEM) and X-ray absorption near edge structure (XANES) analyses of 0.10 wt% Au/TiO₂-A showed that the

state of 0.10 wt% Au/TiO₂-A hardly changed before and after the reaction (Fig. S6–8†). In addition, inductively coupled plasma (ICP) analysis of the filtrate showed no leaching of the Au species into the reaction mixture, demonstrating the high durability of 0.10 wt% Au/TiO₂-A.

In view of the recognized advantages of continuous processing, the reductive conversion of FFA was also tested in a continuous-flow system with a trickle bed reactor utilizing 0.10 wt% Au/TiO₂-A as the packed catalyst under identical conditions (160 °C, 4 MPa H₂; see the ESI†). It turned out that the results obtained from a continuous flow reactor were almost identical to those from a conventional stirring batch reactor, in which the yield of CPO reached 99%. Although a reduction in the yield of CPO from 99% to 95% occurred after 180 h on stream in the reductive conversion of FFA, it was seen that the activity of the slightly-deactivated 0.10 wt% Au/TiO₂-A catalyst could be fully recovered after the treatment in a methanol flow (Fig. 4). As a result, the turnover number (TON) after 540 h under this condition approached 1 000 000, a notably higher number as compared with typical Au-based catalysts.¹⁴ The continuous-flow method described here indicates that this process can be feasible with up to 426 kg of CPO produced per gram of gold with a striking stability of the catalyst over a period of three weeks. Hence this procedure holds great potential for immediate implementation on a larger scale, hereby taking us a step closer to more affordable CPO with benefits of not only providing a compelling alternative approach to produce high value-added chemical products from renewable resources but also of laying a solid foundation for the development of supported Au as a new type of highly efficient heterogeneous catalyst for fixed-bed reactions.

Finally, bearing in mind that current industrial CPO production relies overwhelmingly on the decarboxylation of adipic acid (AA),^{5b,c} we were intrigued by the possibility of exploiting the corresponding reverse reaction (Scheme 2) to make AA. As one of the most in demand commodity chemicals, AA is

Table 3 The hydrogenative rearrangement of other furfural derivatives into the corresponding substituted cyclopentanones^a

Entry	Substrate	<i>t</i> [h]	Conv. [%]	Sel. ^b [%]	
1		2.5	98		99
2		4	97		98
3		8	99		97
4		10	98		96

^a Reaction conditions: catalyst (0.10 wt% Au/TiO₂-A), S/C (2000), H₂O (10 mL), H₂ (4 MPa), 160 °C. ^b The selectivity was based on main products.

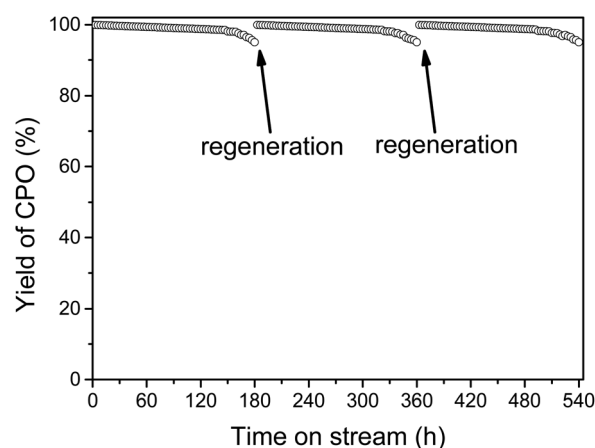
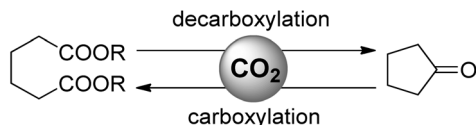


Fig. 4 A continuous-flow transformation of FFA into CPO in a fixed-bed reactor. Reaction conditions: 0.10 wt% Au/TiO₂-A (0.5 g), 160 °C, WHSV (1 h⁻¹), H₂ (4 MPa) flow rate 50 mL min⁻¹.



Scheme 2 The commercial decarboxylation process to produce CPO from DAP and the reverse “carboxylation” of CPO to form DAP.

known to be a versatile building block for a variety of commercially useful products that have found numerous applications in pharmaceuticals, agrochemicals and material science.¹⁵ Presently, AA is mainly produced from several petroleum-based feedstocks (e.g., phenol, benzene, and cyclohexane),¹⁶ but a paradigm shift towards sustainability calls for its widespread production from alternative resources. Despite notable recent efforts, the development of a straightforward and efficient route to AA from abundant renewable sources has remained an ongoing challenge.¹⁷ Within this context, any new processes that can utilize bio-sourced feedstocks and CO₂ simultaneously are highly desirable. Adopting DMC as a logical source of CO₂,¹⁸ we have evaluated the condensation reaction of a series of CPO–DMC mixtures in the presence of various forms of nanostructured CeO₂ as the solid base catalysts.¹⁹ As shown in Table 4, it is possible to obtain DAP with excellent yields (up to 85%) by using {100}/{110} surface-exposed ceria nanorods as the catalyst.²⁰ This result is remarkable, and

Table 4 Synthesis of DAP *via* a condensation and ring-opening reaction between CPO and DMC over various solid bases^a

Entry	Catalyst	Conv. [%]	Sel. [%]			
			DAP	a	b	c
1	MgO	77	61	6	13	19
2	Mg ₃ Al-HT	94	35	13	46	5
3	CeO ₂ -90	58	76	15	2	6
4	CeO ₂ -nanorod	76	83	8	1	7
5	CeO ₂ -meso	44	64	18	1	16
7	CeO ₂ -cube	33	48	17	2	32
8	CeO ₂ -nps	56	54	16	3	26
9	CeO ₂ -octahedra	26	33	27	2	37
10 ^b	CeO ₂ -nanorod	97	87	7	1	4
11 ^{b,c}	CeO ₂ -nanorod	95	84	7	1	7
12 ^{b,d}	CeO ₂ -nanorod	96	85	8	1	5

^a Reaction conditions: CPO (5.6 mmol), DMC (20 mL), N₂ (0.5 MPa), 260 °C, 3 h. ^b 5 h. ^c The third time reused. ^d The reaction feed for DAP production was obtained *via* an extraction of the continuous-flow produced CPO–H₂O stream using DMC, see the ESI for details.

becomes more relevant as an integrated conversion of the continuous-flow produced CPO stream for tandem FFA-to-DAP production was also possible (Table 4, entry 12). With the development of improved methods for DMC synthesis *via* reacting CO₂ with the recycled methanol, this new non-petroleum-based route has the potential to significantly reduce the carbon footprint of AA production processes.

Conclusions

In summary, we have identified a versatile Au-based catalyst that represents by far the most selective and efficient system to date capable of quantitatively converting FFA to CPO. Key to the successful development of this transformation was the use of a unique Au–TiO₂ cooperative catalytic system and the inherently low concentration of the FAL formed in the initial FFA hydrogenation step. Whereas this finding opens new possibilities to produce substituted cyclopentanones from other furanic derivatives at a large scale, the direct access to DAP from a CPO–DMC mixture showcases the feasibility of using biogenic CPO in the synthesis of industrially important feedstocks. Beyond the potential utility of this new system, we anticipate that the general strategy for precisely manipulating complex pathways by exploiting the interplay between Au and the underlying support could be adopted to substantially improve a set of other gold-catalyses, thereby facilitating the application of gold catalysis on an industrial scale, and it might also be helpful for advancing the cooperative catalysis mediated by other transition metals.

Experimental

Catalyst preparation

Preparation of anatase (TiO₂-A), rutile (TiO₂-R), Au/Nb₂O₅, Au/H-ZSM-5, Au/HY, Au/ZrO₂, Au/SiO₂, Au/TiO₂, Au/CeO₂ and Au/HT. All the supports and catalysts were prepared by previously reported methods.^{8a,9,21} The BET surface area of TiO₂-A and TiO₂-R are 146 m² g⁻¹ and 68 m² g⁻¹, respectively.

Preparation of Au/TiO₂-A, Au/TiO₂-R and Au/TiO₂-P25 catalyst. The Au/TiO₂-A catalyst was prepared by a modified deposition–precipitation (DP) method.^{8f,21d} Briefly, an appropriate amount of aqueous solution of HAuCl₄ was heated to 80 °C under vigorous stirring. The pH was adjusted to 7.0 by dropwise addition of NaOH (0.2 M), and then 1.0 g TiO₂-A was dispersed in the solution. After that, the pH was readjusted to 7.0 by dropwise addition of NaOH (0.2 M). The mixture was stirred for 2 h at 80 °C, after which the suspension was cooled to 25 °C. Extensive washing with deionized water was then followed until it was free of chloride ions. The samples were dried under vacuum at 25 °C for 12 h and then calcined in air at 350 °C for 2 h. A similar Au/TiO₂-R catalyst and Au/TiO₂-P25 were prepared by using the same method as that for Au/TiO₂-A. Elemental analysis (ICP-AES) results revealed that the real gold loading was 0.73 wt%, 0.63 wt% and 0.62 wt% for Au/

TiO₂-A, Au/TiO₂-R and Au/TiO₂-P25, respectively. The larger particle sized Au/TiO₂-A was prepared at higher calcined temperatures (450 °C and 550 °C, respectively).

Preparation of Ir/TiO₂-A, Pd/TiO₂-A, Pt/TiO₂-A, Ru/TiO₂-A catalysts. 0.73 wt% Ir/TiO₂-A, 0.73 wt% Pd/TiO₂-A, 0.73 wt% Pt/TiO₂-A, 0.73 wt% Ru/TiO₂-A catalysts were prepared by incipient-wetness impregnation (IWI) of the support with aqueous solutions of H₂IrCl₆·6H₂O, PdCl₂, H₂PtCl₆·6H₂O or RuCl₃ precursors of appropriate concentrations, respectively.^{8f} After a perfect mixing of the corresponding slurries, the resulting mixture was vigorously stirred at 80 °C for 4 h. Then samples were dried under vacuum at 25 °C for 12 h and then reduced in 5 vol% H₂/Ar (80 mL min⁻¹) at 400 °C for 2 h.

Preparation of CeO₂. The various forms of nanostructured CeO₂ were prepared by a procedure described previously.¹⁹ CeO₂ nanorods, nano-octahedra and nanocubes were prepared by the hydrolysis of Ce(III) salts in alkaline medium, followed by a hydrothermal treatment. For the synthesis of CeO₂ nanorods, 3.47 g of Ce(NO₃)₃·6H₂O and 50.4 g of NaOH were first dissolved in 20 and 140 mL of deionized water, respectively. Then, these two aqueous solutions were mixed together in a Teflon bottle, and the mixture was kept stirring for 30 min with the formation of a milky suspension. Subsequently, the Teflon bottle with this suspension was placed in a stainless steel autoclave and subjected to hydrothermal (HT) treatment at 100 °C for 24 h. The same procedures and conditions were adopted for the synthesis of CeO₂ nanocubes except for the amount of NaOH (33.6 g) and the HT temperature (180 °C). For the synthesis of CeO₂ nano-octahedra, 0.868 g Ce(NO₃)₃·6H₂O and 0.0076 g Na₃PO₄·12H₂O were first dissolved in 80 mL of deionized water. After being stirred at 25 °C for 1 h, the mixed solution was transferred into a Teflon-lined stainless steel autoclave and then was subjected to HT treatment at 200 °C for 20 h. After the HT treatment in each case, the solid products were recovered by centrifugation, washed with deionized water and ethanol several times, followed by drying at 60 °C in air overnight. Finally, the solid sample was calcined at 600 °C in air for 6 h.

Catalyst characterization

Elemental analysis. The metal loading of the catalysts was measured by inductively coupled plasma atomic emission spectroscopy (ICP-AES) using a Thermo Electron IRIS Intrepid II XSP spectrometer.

BET analysis. The BET specific surface areas of the prepared catalysts were determined by adsorption–desorption of nitrogen at liquid nitrogen temperature, using Micromeritics TriStar 3000 equipment. Sample degassing was carried out at 300 °C prior to acquiring the adsorption isotherm.

X-ray diffraction (XRD). The crystal structures of various catalysts were characterized with powder X-ray diffraction (XRD) on a Bruker D8 Advance X-ray diffractometer using the Ni-filtered Cu K α radiation source at 40 kV and 40 mA.

Transmission electron microscopy (TEM). TEM images of various catalysts were taken with a JEOL 2011 electron microscope operating at 200 kV. Before being transferred into the

TEM chamber, the samples dispersed with ethanol were deposited onto a carbon-coated copper grid and then quickly moved into the vacuum evaporator. The size distribution of the metal particles was determined by measuring about 200 random particles on the images.

X-ray absorption fine structure (XAFS). The X-ray absorption data at the Au L₃-edge of the samples were recorded at 25 °C in the transmission mode using ion chambers or in the fluorescent mode with a silicon drift fluorescence detector at beam line BL14W1 of the Shanghai Synchrotron Radiation Facility (SSRF), China. The station was operated with a Si (311) double crystal monochromator. During the measurement, the synchrotron was operated at an energy of 3.5 GeV and a current between 150–210 mA. The photon energy was calibrated with standard Pt metal foil. Data processing was performed using the program ATHENA.²²

NH₃-temperature-programmed desorption (NH₃-TPD). NH₃ was adsorbed at 60 °C for 0.5 h after pretreatment at 300 °C for 1 h in a He stream. The desorbed NH₃ in flowing He gas was quantified (NH₂ fragment of mass number 16) by mass spectroscopy (Balzers OmniStar) at 60–700 °C (ramp rate, 10 °C min⁻¹).

Infrared spectra of pyridine adsorption (Py-FTIR). The results were recorded on a Nicolet NEXUS 670 FT-IR spectrometer. The samples were pressed into self-supporting disks and placed in an IR cell attached to a closed glass-circulation system. The disk was pretreated by heating at 400 °C for 1 h under vacuum. After the cell was cooled down to 25 °C, the IR spectrum was recorded as the background. Pyridine vapor was then introduced into the cell at room temperature and heated to 200 °C until equilibrium was reached, and then a second spectrum was recorded. The spectra presented were obtained by subtracting the spectra recorded before and after pyridine adsorption.

Catalytic activity measurements

General procedure for the hydrogenative rearrangement of FFA to CPO. A mixture of FFA (5.2 mmol), supported metal catalysts (metal 0.05 mol% or 0.01 mol%), and water (10 mL) was charged into a 50 mL Hastelloy-C high pressure Parr reactor. The reactant mixtures were then stirred at a rate of 800 rpm under 4 MPa H₂ for a certain reaction time at a given temperature. After reaction, the H₂ atmosphere was removed and the resultant product mixtures were transferred into 20 mL of ethanol. A certain amount of *N,N*-dimethylformamide was then added as an internal standard substance. The samples were analyzed on a Shimadzu GC-17A gas chromatograph equipped with a capillary column HP-FFAP (30 m \times 0.25 mm) and a FID detector. The identification of the products was performed by using a GC-MS spectrometer.

For kinetic studies on hydrogenative rearrangement of FFA, the reaction was conducted by carefully controlling the progress of the reaction at 160 °C under 4 MPa H₂ within a time span of 1 min to 15 hours. The product development and distribution were monitored as a function of reaction time by

analyzing the resultant product mixtures of each of the corresponding experiments.

Procedure for a 50 mmol scale transformation of FFA to CPO and recycling experiments. A mixture of furfural (50 mmol), 0.10 wt% Au/TiO₂-A (metal: 0.005 mol% Au), and water (100 mL) was charged into an autoclave (500 mL capacity) and heated to a certain temperature in less than 15 minutes. The reactant mixtures were then stirred at a rate of 800 rpm under 4 MPa H₂ at a given temperature. After 14 or 15 hours of reaction, the reaction mixture was transferred into 200 mL of ethanol and the catalyst was filtered and washed thoroughly with methanol. The catalyst was then dried under vacuum at 25 °C for 12 h. In the subsequent five successive reused cycles, the yield of CPO was >99%, >99%, 99%, 99% and 99%, respectively.

Procedure for the hydrogenative rearrangement of FFA in a continuous-flow reactor. The transformation of FFA to CPO was also carried out in a vertical fixed-bed reactor. The catalyst was pelletized and sieved to 40–60 mesh size. Then, 0.5 g of the catalyst (0.10 wt% Au/TiO₂-A) was loaded in a stainless steel tubular reactor with an inner diameter of 5 mm and a length of 500 mm. The reaction was operated at 160 °C and 4 MPa H₂, with a gas-flow of 50 mL min⁻¹. The feedstock comprising a diluted aqueous solution of FFA (5 wt%) was continuously introduced into the reactor by an HPLC pump with a WHSV of 1 h⁻¹. The products were obtained when the reaction reached the steady state. The liquid and gas products were cooled and collected in a gas-liquid separator immersed in an ice-water trap. The liquid products were analyzed on a Shimadzu GC-17A gas chromatograph equipped with a capillary column HP-FFAP (30 m × 0.25 mm) and FID. The activity of the spent Au/TiO₂-A catalyst can be recovered by treatment in a methanol flow. Specifically, the slightly deactivated catalyst in the fixed-bed reactor was washed with methanol flow (1 mL min⁻¹) for 60 min.

General procedure for the synthesis of DAP from CPO and DMC. A mixture of CPO (0.5 mL), solid base catalysts (200 mg), and DMC (20 mL) was charged into a 50 mL Hastelloy-C high pressure Parr reactor. The reactant mixtures were then stirred at a rate of 800 rpm under 0.5 MPa N₂ for a certain reaction time at 260 °C. After reaction, the liquid products were added with an internal standard and then analyzed on a Shimadzu GC-17A gas chromatograph equipped with a capillary column HP-FFAP (30 m × 0.25 mm) and a FID detector. The identification of the products was performed by using a GC-MS spectrometer.

The possibility of a tandem FFA-to-DAP production *via* an integrated catalytic conversion of bio-derived FFA-to-CPO coupled with subsequent DAP production was also explored (Table 2, entry 12). Typically 11 g of the continuous-flow produced CPO-water stream (the weight ratio of CPO to water in this mixture was 100:4.5 based on GC analysis) was transferred to a 50 mL round-bottomed flask that contained 20 mL DMC and subjected to vigorous stirring for 1 hour at 25 °C. The bottom solution comprising the hydrophobic CPO-DMC mixture separated spontaneously from the aqueous solution

after extraction. Then to the resultant CPO-DMC mixture was added the CeO₂-nanorod catalyst (200 mg). The reactant mixtures were then transferred to a 50 mL Hastelloy-C high pressure Parr reactor and subjected to reaction at 260 °C for 5 h.

Acknowledgements

This work was supported by the National Natural Science Foundation of China (21273044, 21473035), the Research Fund for the Doctoral Program of Higher Education (20120071110011) and the Science & Technology Commission of Shanghai Municipality (08DZ2270500 and 12ZR1401500).

Notes and references

- (a) B. Kamm, P. R. Grube and M. Kamm, *Biorefineries-Industrial Processes and Products, Status Quo and Future Directions*, Wiley-VCH, Weinheim, 2006, vol. 1; (b) G. W. Huber, S. Iborra and A. Corma, *Chem. Rev.*, 2006, **106**, 4044; (c) A. Corma, S. Iborra and A. Velty, *Chem. Rev.*, 2007, **107**, 2411; (d) P. Gallezot, *Chem. Soc. Rev.*, 2012, **41**, 1538; (e) J. C. Serrano-Ruiz, R. Luque and A. Sepulveda-Escribano, *Chem. Soc. Rev.*, 2011, **40**, 5266; (f) J. A. Melero, J. Iglesias and A. Garcia, *Energy Environ. Sci.*, 2012, **5**, 7393.
- (a) K. J. Zeitsch, *The chemistry and technology of furfural and its many by-products*, Elsevier B.V., 2000, vol. 13; (b) R. Karinen, K. Vilonen and M. Niemelä, *ChemSusChem*, 2011, **4**, 1002; (c) J. P. Lange, E. van der Heide, J. van Buijtenen and R. Price, *ChemSusChem*, 2012, **5**, 150; (d) Y. Nakagawa, M. Tamura and K. Tomishige, *ACS Catal.*, 2013, **3**, 2655; (e) C. M. Cai, T. Y. Zhang, R. Kumara and C. E. Wyman, *J. Chem. Technol. Biotechnol.*, 2014, **89**, 2; (f) B. Danon, G. Marcotullio and W. de Jong, *Green Chem.*, 2014, **16**, 39.
- (a) B. J. Liu, L. H. Lu, B. C. Wang, T. X. Cai and I. Katsuyoshi, *Appl. Catal., A*, 1998, **171**, 117; (b) J. G. Stevens, R. A. Bourne, M. V. Twigg and M. Poliakoff, *Angew. Chem., Int. Ed.*, 2010, **49**, 8856; (c) S. Sitthisa, W. An and D. E. Resasco, *J. Catal.*, 2011, **284**, 90; (d) N. Alonso-Fagúndez, M. L. Granados, R. Mariscal and M. Ojeda, *ChemSusChem*, 2012, **5**, 1984; (e) Y. Nakagawa, H. Nakazawa, H. Watanabe and K. Tomishige, *ChemCatChem*, 2012, **4**, 1791; (f) S. B. Liu, Y. Amada, M. Tamura, Y. Nakagawa and K. Tomishige, *Green Chem.*, 2014, **16**, 617; (g) F. Dong, Y. L. Zhu, G. Q. Ding, J. L. Cui, X. Q. Li and Y. W. Li, *ChemSusChem*, 2015, **8**, 1534.
- (a) M. Hronec and K. Fulajtarová, *Catal. Commun.*, 2012, **24**, 100; (b) M. Hronec, K. Fulajtarová and T. Liptaj, *Appl. Catal., A*, 2012, **437**, 104; (c) Y. L. Yang, Z. T. Du, Y. Z. Huang, F. Lu, F. Wang, J. Gao and J. Xu, *Green Chem.*, 2013, **15**, 1932; (d) M. Hronec, K. Fulajtarová and

- M. Micušik, *Appl. Catal., A*, 2013, **468**, 426; (e) X. L. Li, J. Deng, T. Pan, C. G. Yu, H. J. Xu and Y. Fu, *Green Chem.*, 2015, **17**, 1038; (f) H. Y. Zhu, M. H. Zhou, Z. Zeng, G. M. Xiao and R. Xiao, *Korean J. Chem. Eng.*, 2014, **31**, 593; (g) C. Y. Liu, R. P. Wei, G. L. Geng, M. H. Zhou, L. J. Gao and G. M. Xiao, *Fuel Process. Technol.*, 2015, **134**, 168; (h) R. Q. Fang, H. L. Liu, R. Luque and Y. W. Li, *Green Chem.*, 2015, **17**, 4183; (i) M. Hronec, K. Fulajtarová, I. Vávra, T. Soták and E. Dobročka, *Appl. Catal., B*, 2016, **181**, 210.
- 5 (a) M. Renz, *Eur. J. Org. Chem.*, 2005, 979; (b) O. Nagashima, S. Sato, R. Takahashi, T. Sodesawa and T. Akashi, *Appl. Catal., A*, 2006, **312**, 175; (c) P. Sudarsanam, L. Katta, G. Thrimurthulu and B. M. Reddy, *J. Ind. Eng. Chem.*, 2013, **19**, 1517; (d) M. Hronec, K. Fulajtarová, T. Liptaj, M. Štolcová, N. Prónayová and T. Soták, *Biomass Bioenergy*, 2014, **63**, 291; (e) J. F. Yang, N. Li, G. Y. Li, W. T. Wang, A. Q. Wang, X. D. Wang, Y. Cong and T. Zhang, *Chem. Commun.*, 2014, **50**, 2572.
- 6 (a) G. Piancatelli, A. Scettri, G. David and M. Dauria, *Tetrahedron*, 1978, **34**, 2775; (b) O. N. Faza, C. S. López, R. Álvarez and Á. R. de Lera, *Chem. – Eur. J.*, 2004, **10**, 4324; (c) G. K. Veits, D. R. Wenz and J. R. de Alaniz, *Angew. Chem., Int. Ed.*, 2010, **49**, 9484; (d) M. Masayoshi, *US Patent*, 4970345, 1990.
- 7 (a) C. Mohr, H. Hofmeister, J. Radnik and P. Claus, *J. Am. Chem. Soc.*, 2003, **125**, 1905; (b) A. Corma and P. Serna, *Science*, 2006, **313**, 332; (c) A. Negoii, S. Wuttke, E. Kemnitz, D. Macovei, V. I. Parvulescu, C. M. Teodorescu and S. M. Coman, *Angew. Chem., Int. Ed.*, 2010, **49**, 8134; (d) G. Li, C. Zeng and R. Jin, *J. Am. Chem. Soc.*, 2014, **136**, 3673.
- 8 (a) L. He, L. C. Wang, H. Sun, J. Ni, Y. Cao, H. Y. He and K. N. Fan, *Angew. Chem., Int. Ed.*, 2009, **48**, 9538; (b) D. Ren, L. He, R. L. S. Ding, Y. M. Liu, Y. Cao, H. Y. He and K. N. Fan, *J. Am. Chem. Soc.*, 2012, **134**, 17592; (c) X. Liu, L. He, Y. M. Liu and Y. Cao, *Acc. Chem. Res.*, 2014, **47**, 793; (d) S. S. Li, X. Liu, Y. M. Liu, H. Y. He, K. N. Fan and Y. Cao, *Chem. Commun.*, 2014, **50**, 5626; (e) X. Liu, H. Q. Li, S. Ye, Y. M. Liu, H. Y. He and Y. Cao, *Angew. Chem., Int. Ed.*, 2014, **53**, 7624; (f) L. Yu, Q. Zhang, S. S. Li, J. Huang, Y. M. Liu, H. Y. He and Y. Cao, *ChemSusChem*, 2015, **8**, 3029.
- 9 J. Ohyama, R. Kanao, A. Esakia and A. Satsuma, *Chem. Commun.*, 2014, **50**, 5633.
- 10 An evaluation of the acidic properties by NH₃-temperature-programmed desorption (NH₃-TPD, Fig. S2†) coupled with IR spectroscopic measurement of adsorbed pyridine (Fig. S3†) revealed that TiO₂-A possesses only mild Lewis acidic sites with a much lower population density as compared to other supports, thus verifying the distinguished bifunctional character of the Au/TiO₂-A catalyst.
- 11 We have confirmed in a set of separate experiments that the TiO₂-A supported Pt and Pd NPs exhibited much higher intrinsic FFA hydrogenation activity than Au/TiO₂-A at 80 °C (Table S3†). It is therefore reasonable to assume that, as a consequence of the undesired decarbonylation pathway that occurred under the conditions of the standard assay, a trace amount of the resultant CO can severely restrict the ability of PGM-based catalysts to initiate FFA conversion.
- 12 (a) A. Kulkarni and B. Török, *Curr. Org. Synth.*, 2011, **8**, 187; (b) M. Irfan, T. N. Glasnov and C. O. Kappe, *ChemSusChem*, 2011, **4**, 300; (c) J. Pritchard, G. A. Filonenko, R. van Putten, E. J. M. Hensen and E. A. Pidko, *Chem. Soc. Rev.*, 2015, **44**, 3808.
- 13 Selected examples of recent reports using TiO₂ as an efficient water-compatible heterogeneous Lewis acid catalyst: (a) K. Nakajima, R. Noma, M. Kitano and M. Hara, *J. Phys. Chem. C*, 2013, **117**, 16028; (b) R. Noma, K. Nakajima, K. Kamata, M. Kitano, S. Hayashi and M. Hara, *J. Phys. Chem. C*, 2015, **119**, 17117; (c) H. Hirakawa, M. Katayama, Y. Shiraishi, H. Sakamoto, K. L. Wang, B. Ohtani, S. Ichikawa, S. Tanaka and T. Hirai, *ACS Appl. Mater. Interfaces*, 2015, **7**, 3797.
- 14 (a) J. Oliver-Meseguer, J. R. Cabrero-Antonionio, I. Domínguez, A. Leyva-Pérez and A. Corma, *Science*, 2012, **338**, 1452; (b) M. C. B. Jaimes, C. R. N. Böhlring, J. M. Serrano-Becerra and A. S. K. Hashmi, *Angew. Chem., Int. Ed.*, 2013, **52**, 7963.
- 15 (a) K. Weissermel and H.-J. Arpe, *Industrial Organic Chemistry*, Wiley-VCH, Weinheim, 2003; (b) A. Castellan, J. C. J. Bart and S. Cavallaro, *Catal. Today*, 1991, **9**, 237.
- 16 (a) K. Sato, M. Aoki and R. Noyori, *Science*, 1998, **281**, 1646; (b) S. O. Lee, R. Raja, K. D. M. Harris, J. M. Thomas, B. F. G. Johnson and G. Sankar, *Angew. Chem., Int. Ed.*, 2003, **42**, 1520; (c) S. Van de Vyver and Y. Román-Leshkov, *Catal. Sci. Technol.*, 2013, **3**, 1465.
- 17 (a) T. Polen, M. Spelberg and M. Bott, *J. Biotechnol.*, 2013, **167**, 75; (b) R. Beerthuis, G. Rothenberg and N. R. Shiju, *Green Chem.*, 2015, **17**, 1341.
- 18 (a) J. Bian, M. Xiao, S. J. Wang, Y. X. Lu and Y. Z. Meng, *Catal. Commun.*, 2009, **10**, 1142; (b) D. Ballivet-Tkatchenko, F. Bernard, F. Demoisson, L. Plasseraud and S. R. Sanapureddy, *ChemSusChem*, 2011, **4**, 1316; (c) A. Bansode and A. Urakawa, *ACS Catal.*, 2014, **4**, 3877.
- 19 (a) H. X. Mai, L. D. Sun, Y. W. Zhang, R. Si, W. Feng, H. P. Zhang, H. C. Liu and C. H. Yan, *J. Phys. Chem. B*, 2005, **109**, 24380; (b) J. L. He, T. Xu, Z. H. Wang, Q. H. Zhang, W. P. Deng and Y. Wang, *Angew. Chem., Int. Ed.*, 2012, **51**, 2438.
- 20 Although we are aware that there is one precedent of subjecting the CPO–DMC mixture to MgO, we emphasize that in this case only a modest yield (<40%) of DAP was attainable: (a) D. D. Wu, Z. Chen, Z. B. Jia and L. Shuai, *Sci. China: Chem.*, 2012, **55**, 380.
- 21 (a) X. Zhang, H. Shi and B. Q. Xu, *Angew. Chem., Int. Ed.*, 2005, **44**, 7132; (b) X. L. Du, L. He, S. Zhao, Y. M. Liu, Y. Cao, H. Y. He and K. N. Fan, *Angew. Chem., Int. Ed.*, 2011, **50**, 7815; (c) Q. Y. Bi, X. L. Du, Y. M. Liu, Y. Cao,

- H. Y. He and K. N. Fan, *J. Am. Chem. Soc.*, 2012, **134**, 8926; (d) L. Tao, Q. Zhang, S. S. Li, X. Liu, Y. M. Liu and Y. Cao, *Adv. Synth. Catal.*, 2015, **357**, 753; (e) M. M. Wang, L. He, Y. M. Liu, Y. Cao, H. Y. He and K. N. Fan, *Green Chem.*, 2011, **13**, 602; (f) L. J. Liu, H. L. Zhao, J. M. Andino and Y. Li, *ACS Catal.*, 2012, **2**, 1817; (g) C. Sun, Y. S. Yang, J. M. Du, F. Qin, Z. P. Liu, W. Shen, H. L. Xu and Y. Tang, *Chem. Commun.*, 2012, **48**, 5787.
- 22 B. Ravel and M. Newville, *J. Synchrotron Radiat.*, 2005, **71**, 6652.